

Spatiotemporal Modeling of Multivariate Signals with Graph Neural Networks and Structured State Space Models

Siyi Tang, Jared A. Dunnmon, Liangqiong Qu, Khaled K. Saab,
Christopher Lee-Messer, Daniel L. Rubin

Stanford University

{siyitang,jdunnmon,liangqi,ksaab,cleemess,rubin}@stanford.edu

Abstract

Multivariate signals are prevalent in various domains, such as healthcare, transportation systems, and space sciences. Modeling spatiotemporal dependencies in multivariate signals is challenging due to (1) long-range temporal dependencies and (2) complex spatial correlations between sensors. To address these challenges, we propose representing multivariate signals as graphs and introduce GRAPH4MER, a general graph neural network (GNN) architecture that captures both spatial and temporal dependencies in multivariate signals. Specifically, (1) we leverage Structured State Spaces model (S4), a state-of-the-art sequence model, to capture long-term temporal dependencies and (2) we propose a graph structure learning layer in GRAPH4MER to learn dynamically evolving graph structures in the data. We evaluate our proposed model on three distinct tasks and show that GRAPH4MER consistently improves over existing models, including (1) seizure detection from electroencephalography signals, outperforming a previous GNN with self-supervised pretraining by 3.1 points in AUROC; (2) sleep staging from polysomnography signals, a 4.1 points improvement in macro-F1 score compared to existing sleep staging models; and (3) traffic forecasting, reducing MAE by 8.8% compared to existing GNNs and by 1.4% compared to Transformer-based models.

1 Introduction

Multivariate signals are time series data measured by multiple sensors and are prevalent in many real-world applications, including healthcare [50], transportation systems [20], power systems [51], and space sciences [10]. An example multivariate signal is scalp electroencephalograms (EEGs), which measure brain electrical activities using sensors placed on an individual’s scalp.

Several challenges exist in modeling spatiotemporal dependencies in multivariate signals. First, many types of signals are sampled at a high sampling rate, which results in long sequences that can be up to tens of thousands of time steps. Moreover, multivariate signals often involve long-range temporal correlations [7]. Prior studies on modeling long signals often preprocess the raw signals using frequency transformations [4, 15, 32, 33, 63, 66] or divide the signals into short windows and aggregate model predictions post-hoc [55, 56]. However, such preprocessing steps may discard important information encoded in raw signals, as well as neglect long-range temporal dependencies in the signals. Therefore, a model that is capable of modeling long-range temporal correlations in raw signals is needed.

Deep sequence models, including recurrent neural networks (RNNs), convolutional neural networks (CNNs), and Transformers, have specialized variants for handling long sequences [3, 14, 19, 42]. However, they struggle to scale to long sequences of tens of thousands of time steps [67]. Recently, the Structured State Space sequence model (S4) [31], a deep sequence model based on the classic state space model, has achieved state-of-the-art performance on challenging long sequence modeling tasks, such as the Long Range Arena benchmark [67], raw speech classification [31], and audio generation [27].

Second, sensors have complex, non-Euclidean spatial correlations. For example, EEG sensors measure highly correlated yet unique electrical activities from different brain regions [49]; traffic speeds

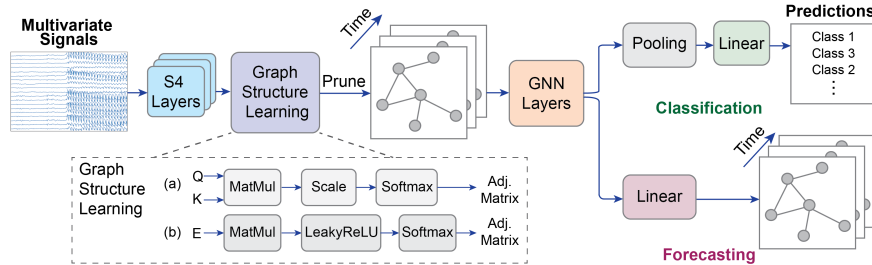


Figure 1: **Architecture of GraphS4mer.** The model has three main components: (1) stacked S4 layers to learn temporal dependencies in each sensor independently; (2) a graph structure learning (GSL) layer to learn dynamically evolving graph structures; (3) GNN layers to learn spatial dependencies based on S4 embeddings and learned graph structures. For GSL, we adopt (a) self-attention and (b) a learnable embedding for inductive and transductive settings, respectively.

are correlated not only based on physical distances between traffic sensors, but also dependent on the traffic flows [45]. Graphs are data structures that can model complex, non-Euclidean correlations in the data [8, 11]. Previous works have adopted temporal graph neural networks (GNNs) in modeling multivariate time series, such as EEG-based seizure detection [15] and classification [66], traffic forecasting [38, 45, 68, 71, 78], and pandemic forecasting [41, 53]. Nevertheless, most of these studies use sequences up to hundreds of time steps and require a predefined, static graph structure. However, the graph structure of multivariate signals may not be easily defined due to unknown sensor locations. For instance, while EEG sensors are typically placed according to the 10-20 standard placement [36], the exact locations of sensors vary in each individual’s recordings due to the variability in individual head size. Moreover, the underlying graph connectivity can evolve over time due to temporal dynamics in the data. Hence, when graph structures cannot be easily predefined, the ability to dynamically learn the underlying graph structures is highly desired.

Graph structure learning (GSL) aims to jointly learn an optimized graph structure and its node and graph representations [79]. GSL techniques have been used in non-temporal graph applications, such as natural language processing [73], molecular optimization [22], learning on point clouds [70], and improving GNN robustness against adversarial attacks [39, 75]. GSL has also been employed for spatiotemporal modeling of traffic flows [5, 62, 65, 71, 74], irregularly sampled multivariate time series [76], functional magnetic resonance imaging (fMRI) [18, 26], and sleep staging [37], but they are limited to sequences of less than 1k time steps and do not capture dynamic graph structures evolving over time.

In this study, we address the foregoing challenges by (1) leveraging S4 to enable long-range temporal modeling and (2) proposing a graph structure learning layer to learn dynamically evolving graph structures in multivariate signals. Our main contributions are:

- We propose GRAPH S4MER (Figure 1), a general end-to-end GNN architecture for spatiotemporal modeling of multivariate signals. Our model has two major advantages: (1) it leverages S4 to capture *long-range temporal dependencies* in signals and (2) it is able to *dynamically learn the underlying graph structures* in the data without a predefined graph.
- We evaluate GRAPH S4MER on three datasets with distinct data types and tasks. Our model consistently outperforms existing methods on (1) seizure detection from EEG signals, outperforming a previous GNN with self-supervised pretraining by 3.1 points in AUROC; (2) sleep staging from polysomnography signals, outperforming existing sleep staging models by 4.1 points in macro-F1 score; (3) traffic forecasting on PEMS-BAY benchmark, reducing MAE by 8.8% compared to existing GNNs and by 1.4% compared to Transformers.
- Qualitative interpretability analysis suggests that our GSL method learns meaningful graph structures that reflect the underlying seizure classes and sleep stages.

2 Related Works

Temporal graph neural networks. Temporal GNNs have been widely used for multivariate time series. A recent work by Gao and Ribeiro [23] shows that existing temporal GNNs can be grouped into two categories: time-and-graph and time-then-graph. The time-and-graph framework treats a temporal graph as a sequence of graph snapshots, constructs a graph representation for each snapshot, and embeds the temporal evolution using sequence models. For example, GCRN [60] uses spectral graph convolution [17] for node representations and Long Short-Term Memory network (LSTM) [34] for temporal dynamics modeling. DCRNN [45] integrates diffusion convolution with Gated Recurrent Units (GRU) [13] for traffic forecasting. Li et al. [43] combines relational graph convolution with LSTM for path failure prediction. EvolveGCN [54] treats graph convolutional network (GCN) parameters as recurrent states and uses an recurrent neural network (RNN) to evolve the GCN parameters. In contrast, time-then-graph framework sequentially represents the temporal evolution of node and edge attributes, and uses these temporal representations to build a static graph representation [16, 58]. Gao and Ribeiro [23] proposes a general framework for time-then-graph, which represents the evolution of node and edge features using two RNNs independently, constructs a static graph from these representations, and encodes them using a GNN. However, most of the existing temporal GNNs are limited to short sequences and adopt RNNs or self-attention for temporal modeling, which may be suboptimal when applied to long sequences. To our knowledge, only one study has leveraged S4 for temporal graphs [25]. However, the learned graph is static and shared across all data points, and it is limited to fMRI data.

Graph structure learning. GSL aims to jointly learn a graph structure and its corresponding node (or graph) representations. Briefly, GSL methods fall into the following three categories [79]: (1) metric-based approaches that derive edge weights from node embeddings based on a metric function [12, 44, 75], (2) neural-based approaches that use neural networks to learn the graph structure from node embeddings [37, 48, 77], and (3) direct approaches that treat the adjacency matrix or node embedding dictionary as learnable parameters [24, 39]. GSL has been applied to temporal graph data. Zhang et al. [74] proposes learning graph adjacency matrix from traffic data through learnable parameters. Tang et al. [65] uses a multi-layer perceptron and a similarity measure to learn the graph structure for traffic forecasting. Shang et al. [62] leverages a link predictor (two fully connected layers) to obtain the edge weights. Several works adaptively learn the adjacency matrix from data using learnable node embedding dictionaries [18, 25, 71]. However, these GSL approaches are limited to short sequences of less than 1k time steps and do not capture dynamically evolving graph structures.

3 Background

3.1 Structured State Space model (S4)

The Structured State Space sequence model (S4) [31] is a deep sequence model that is capable of capturing long-range dependencies. S4 has achieved state-of-the-art on pixel-level 1-D image classification, the challenging Long Range Arena benchmark for long sequence modeling, raw speech classification, and audio generation [27, 31].

S4 is based on the state space model (SSM). A recent line of work [29–31] has shown that SSMs can be viewed as both convolutional neural networks (CNNs) and RNNs. The continuous-time SSM is defined as follows, which maps an 1-D signal $u(t)$ to a high dimensional latent state $x(t)$ before projecting to a 1-D output signal $y(t)$:

$$x'(t) = \mathbf{A}x(t) + \mathbf{B}u(t), \quad y(t) = \mathbf{C}x(t) + \mathbf{D}u(t) \quad (1)$$

Equation 1 can be used as a black-box sequence representation in a deep learning model, where \mathbf{A} , \mathbf{B} , \mathbf{C} , and \mathbf{D} are parameters learned by gradient descent. In the rest of this section, \mathbf{D} is omitted for exposition because $\mathbf{D}u(t)$ can be viewed as a skip connection and can be easily computed [31].

Gu et al. [30] shows that discrete-time SSM is equivalent to the following convolution:

$$\overline{\mathbf{K}} := (\overline{\mathbf{C}\mathbf{B}}, \overline{\mathbf{C}\mathbf{A}\mathbf{B}}, \dots, \overline{\mathbf{C}\mathbf{A}^{L-1}\mathbf{B}}), \quad y = \overline{\mathbf{K}} * u \quad (2)$$

where $\overline{\mathbf{A}}$, $\overline{\mathbf{B}}$, and $\overline{\mathbf{C}}$ are the discretized matrices of \mathbf{A} , \mathbf{B} , and \mathbf{C} , respectively; $\overline{\mathbf{K}}$ is called the SSM convolution kernel; and L is the sequence length.

S4 [31] is a special instantiation of SSMs that parameterizes \mathbf{A} as a diagonal plus low-rank (DPLR) matrix. This parameterization has two major advantages. First, it enables fast computation of the SSM kernel $\overline{\mathbf{K}}$. Second, the parameterization includes the HiPPO matrices [29], which are a class of matrices that is capable of capturing long-range dependencies.

However, naively applying S4 for multivariate signals projects the signal channels to the hidden dimension with a linear layer [31], which does not take into account the underlying graph structure of multivariate signals. This motivates our development of GRAPH-S4MER described in Section 4.

3.2 Graph regularization

Graph regularization encourages a learned graph to have several desirable properties, such as smoothness, sparsity, and connectivity [12, 40, 79]. Let $\mathbf{X} \in \mathbb{R}^{N \times D}$ be a graph data with N nodes and D features. First, a common assumption in graph signal processing is that features change smoothly between adjacent nodes [52]. Given an undirected graph with adjacency matrix \mathbf{W} , the smoothness of the graph can be measured by the Dirichlet energy [6]:

$$\mathcal{L}_{\text{smooth}}(\mathbf{X}, \mathbf{W}) = \frac{1}{2N^2} \sum_{i,j} \mathbf{W}_{ij} \|\mathbf{X}_{i,:} - \mathbf{X}_{j,:}\|^2 = \frac{1}{N^2} \text{tr}(\mathbf{X}^T \mathbf{L} \mathbf{X}) \quad (3)$$

where $\text{tr}(\cdot)$ denotes the trace of a matrix, $\mathbf{L} = \mathbf{D} - \mathbf{W}$ is the graph Laplacian, \mathbf{D} is the degree matrix of \mathbf{W} . Minimizing Equation 3 therefore encourages the learned graph to be smooth. In practice, the normalized graph Laplacian $\hat{\mathbf{L}} = \mathbf{D}^{-1/2} \mathbf{L} \mathbf{D}^{-1/2}$ is used so that it is independent of node degrees.

However, simply minimizing the smoothness may result in a trivial solution $\mathbf{W} = \mathbf{0}$ [12]. To avoid this trivial solution and encourage sparsity of the learned graph, additional constraints can be added [12, 40]:

$$\mathcal{L}_{\text{degree}}(\mathbf{W}) = \frac{-1}{N} \mathbf{1}^T \log(\mathbf{W} \mathbf{1}), \quad \mathcal{L}_{\text{sparse}}(\mathbf{W}) = \frac{1}{N^2} \|\mathbf{W}\|_F^2 \quad (4)$$

where $\|\cdot\|_F$ is the Frobenius norm of a matrix. Intuitively, $\mathcal{L}_{\text{degree}}$ penalizes disconnected graphs and $\mathcal{L}_{\text{sparse}}$ discourages nodes with high degrees (i.e., encourages the learned graph to be sparse).

4 Methods

4.1 Problem setup

In this study, we propose a general representation of multivariate signals using graphs. Let $\mathbf{X} \in \mathbb{R}^{N \times T \times M}$ be a multivariate signal, where N is the number of sensors, T is the sequence length, and M is the input dimension of the signal (typically $M = 1$). We represent the multivariate signal as a graph $\mathcal{G} = \{\mathcal{V}, \mathcal{E}, \mathbf{W}\}$, where the set of nodes \mathcal{V} corresponds to the sensors, \mathcal{E} is the set of edges, and \mathbf{W} is the adjacency matrix. Here, \mathcal{E} and \mathbf{W} are unknown and will be learned by our model.

While our formulation is general to any type of node-level or graph-level classification and regression tasks, we focus on graph-level classification (e.g., seizure detection) and node-level forecasting problems (e.g., traffic forecasting) in this work. For graph classification, the goal is to learn a function which maps an input signal to a prediction, i.e., $f : \mathbf{X} \rightarrow y \in \{1, 2, \dots, C\}$, where C is the number of classes. For node-level forecasting, the goal is to learn a function which predicts the next S' time step signals given the previous S time step signals, i.e., $f : \mathbf{X}_{:, (t-S):t,:} \rightarrow \mathbf{X}_{:, t:(t+S'), :}$.

4.2 Temporal modeling with S4

In this work, we leverage S4 to capture long-range temporal dependencies in signals. Naively applying S4 for multivariate signals projects the N signal channels to the hidden dimension with a linear layer [31], which may be suboptimal because it neglects the underlying graph structure of multivariate signals. Instead, we use stacked S4 layers with residual connection to embed signals in each channel (sensor) independently, resulting in an embedding $\mathbf{H} \in \mathbb{R}^{N \times T \times D}$ for each input signal \mathbf{X} , where D is the embedding dimension.

4.3 Dynamic graph structure learning

Graph structure learning layer. To model spatial dependencies in signals (i.e., graph adjacency matrix \mathbf{W}), we develop a graph structure learning (GSL) layer to learn the similarities between nodes. To capture the dynamics of signals that evolve over time, our GSL layer learns a *unique* graph structure within a short time interval r , where r is a pre-specified resolution. Instead of learning a unique graph at each time step, we choose to learn a graph over r time interval because (1) aggregating information across a longer time interval can result in less noisy graphs and (2) it is more computationally efficient. For convenience, we let the predefined resolution r be an integer and assume that the sequence length T is divisible by r without overlaps. In the remainder of this paper, we denote $n_d = \frac{T}{r}$ as the number of dynamic graphs.

For inductive settings where the task is to predict on unseen multivariate signals (e.g., seizure detection), the goal of GSL is to learn a unique graph for each multivariate signal within r time interval. To obtain the edge weight between two nodes, we adopt self-attention [69] to allow each node to attend to all other nodes and use the attention weight as the edge weight:

$$\mathbf{Q} = \mathbf{h}^{(t)}\mathbf{M}^Q, \quad \mathbf{K} = \mathbf{h}^{(t)}\mathbf{M}^K, \quad \overline{\mathbf{W}}^{(t)} = \text{softmax}\left(\frac{\mathbf{Q}\mathbf{K}^T}{\sqrt{D}}\right), \quad \text{for } t = 1, 2, \dots, n_d \quad (5)$$

Here, $\mathbf{h}^{(t)} \in \mathbb{R}^{N \times D}$ is mean-pooled S4 embeddings within time $((t-1) \times r, t \times r]$; $\mathbf{M}^Q \in \mathbb{R}^{D \times D}$ and $\mathbf{M}^K \in \mathbb{R}^{D \times D}$ are weights projecting $\mathbf{h}^{(t)}$ to query \mathbf{Q} and key \mathbf{K} , respectively; $\overline{\mathbf{W}}^{(t)} \in \mathbb{R}^{N \times N}$ is the learned adjacency matrix within time $((t-1) \times r, t \times r]$. Equation 5 can be easily extended to multihead self-attention [69].

For transductive settings where all sensors form a graph (e.g., traffic forecasting), we use a learnable embedding $\mathbf{E}^{(t)} \in \mathbb{R}^{N \times d_e}$ in GSL to learn a graph for all multivariate signals within r time interval [5, 71]:

$$\overline{\mathbf{W}}^{(t)} = \text{softmax}(\text{LeakyReLU}(\mathbf{E}^{(t)}\mathbf{E}^{(t)T})), \quad \text{for } t = 1, 2, \dots, n_d \quad (6)$$

Here, d_e is the embedding dimension, and $\mathbf{E}^{(t)}$ is initialized randomly and trained end-to-end.

There are several advantages of our GSL layer compared to prior works [18, 25, 71]. First, our GSL layer is operated on S4 embeddings rather than raw signals, which leverages the long-range dependencies learned by S4 layers. Second, in inductive settings, our GSL layer learns a dynamic graph within a short time interval r for each multivariate signal rather than a universal, static graph for all multivariate signals. Third, our GSL layer is able to learn dynamically evolving graph structures over time.

To guide the graph structure learning process, we add a k-nearest neighbor (KNN) graph $\mathbf{W}_{\text{KNN}}^{(t)}$ to the learned adjacency matrix $\overline{\mathbf{W}}^{(t)}$, where each node’s k-nearest neighbors are defined by cosine similarity between their respective values in $\mathbf{h}^{(t)}$, and $\mathbf{h}^{(t)}$ is the mean-pooled S4 embeddings within time $((t-1) \times r, t \times r]$:

$$\mathbf{W}^{(t)} = \epsilon \mathbf{W}_{\text{KNN}}^{(t)} + (1 - \epsilon) \overline{\mathbf{W}}^{(t)} \quad (7)$$

where $\epsilon \in [0, 1]$ is a hyperparameter for the weight of the KNN graph.

To introduce graph sparsity, we prune the adjacency matrix $\mathbf{W}^{(t)}$ by removing edges whose weights are smaller than a certain threshold, i.e., $\mathbf{W}_{ij}^{(t)} = 0$ if $\mathbf{W}_{ij}^{(t)} < \kappa$, where κ is a hyperparameter. For undirected graphs, we make the learned adjacency matrix symmetric by taking the average of the edge weights between two nodes.

Graph regularization. To encourage the learned graphs to have desirable graph properties, we include three regularization terms as detailed in Equations 3-4. Let $\mathbf{h}^{(t)} \in \mathbb{R}^{N \times D}$ be the mean-pooled S4 embeddings within $((t-1) \times r, t \times r]$. The regularization loss is the weighted sum of the three regularization terms and averaged across all dynamic graphs: $\mathcal{L}_{\text{reg}} = \frac{1}{n_d} \sum_{t=1}^{n_d} \alpha \mathcal{L}_{\text{smooth}}(\mathbf{h}^{(t)}, \mathbf{W}^{(t)}) + \beta \mathcal{L}_{\text{degree}}(\mathbf{W}^{(t)}) + \gamma \mathcal{L}_{\text{sparse}}(\mathbf{W}^{(t)})$, where α , β , and γ are hyperparameters.

4.4 Model architecture

The overall architecture of our model (Figure 1 and Algorithm 1 in Appendix A), GRAPHSS4MER, consists of three main components: (1) stacked S4 layers with residual connection to model temporal dependencies in signals within each sensor independently, which maps raw signals $\mathbf{X} \in \mathbb{R}^{N \times T \times M}$

to S4 embedding $\mathbf{H} \in \mathbb{R}^{N \times T \times D}$, (2) a GSL layer to learn dynamically evolving adjacency matrices $\mathbf{W}^{(1)}, \dots, \mathbf{W}^{(n_d)}$, and (3) GNN layers to learn spatial dependencies between sensors given the learned graph structures $\mathbf{W}^{(1)}, \dots, \mathbf{W}^{(n_d)}$ and node features \mathbf{H} . While our model is general to any kind of GNN layers, we use an expressive GNN architecture, Graph Isomorphism Network (GIN) [35, 72], in our experiments.

For graph classification tasks, a temporal pooling layer and a graph pooling layer are added to aggregate temporal and spatial representations, respectively, which is followed by a fully connected layer to produce a prediction for each multivariate signal. Whereas for node forecasting tasks, a fully connected layer is added to project the outputs of the GNN layers to the output dimension. The total loss is the sum of the regularization loss and the prediction loss. Figure 1 shows the overall model architecture, and Algorithm 1 in Appendix A shows the pseudocode for GRAPH4MER. Source code is publically available at <https://github.com/tsy935/graphs4mer>.

5 Experiments

5.1 Experimental setup

In this section, we briefly introduce the datasets and experimental setup in our study. For each experiment, we ran three runs with different random seeds and report mean and standard deviation of the results. See Appendix B–C for details on datasets, model training procedures, and hyperparameters.

Seizure detection from EEGs. We first evaluate our model on EEG-based seizure detection. We use the publicly available Temple University Hospital Seizure Detection Corpus (TUSZ) v1.5.2 [61], and follow the experimental setup of seizure detection on 60-s EEG clips as in Tang et al. [66]. The number of EEG sensors is 19. The sampling rate of each 60-s EEG clip is 200 Hz, resulting in a sequence length of 12k time steps. The task is binary classification of detecting whether or not a 60-s EEG clip contains seizure. The resolution r in GSL layer is chosen as 10-s (i.e., 2,000 time steps), which is inspired by how trained EEG readers analyze EEGs. As this is an inductive graph classification task, we adopt Equation 5 for GSL. The EEG graphs are undirected.

We compare our model performance to existing models for seizure detection, including (1) LSTM [34], a variant of RNN with gating mechanisms; (2) Dense-CNN [59], a densely connected CNN specialized in seizure detection; (3) CNN-LSTM [2]; and (4) Dist- and Corr-DCRNN without and with self-supervised pre-training [66]. Following prior studies, we use AUROC as the evaluation metric.

Sleep staging from polysomnography signals. Next, we evaluate our model on sleep staging from polysomnography (PSG) signals. PSG is used in the diagnosis of sleep disorders such as obstructive sleep apnea. We use the publicly available Dreem Open Dataset-Healthy (DOD-H) [33]. We randomly split the data by 60/20/20 into train/validation/test sets, where each split consists of data from distinct subjects. The number of PSG sensors is 16. The sampling rate is 250 Hz, and thus each 30-s signal has 7,500 time steps. The task is to classify each 30-s PSG signal as one of the five sleep stages: wake, rapid eye movement (REM), non-REM sleep stages N1, N2, and N3. The resolution r is 10-s (i.e., 2.5k time steps). This is also an inductive graph classification task, and thus we adopt Equation 5 for GSL. The PSG graphs are undirected.

Baseline models include existing sleep staging models that achieved state-of-the-art on DOD-H dataset, SimpleSleepNet [33] and RobustSleepNet [32], both of which are based on GRUs [13] and attention mechanisms. We also include the traditional sequence model LSTM [34] as a baseline. For fair comparisons between the baselines and GRAPH4MER, we trained SimpleSleepNet and RobustSleepNet using their open sourced code¹ and setting the temporal context to be one 30-s PSG signal. Similar to Guillot and Thorey [32], we use macro-F1 score and Cohen’s Kappa as the evaluation metrics.

Traffic forecasting. Finally, we evaluate our model on forecasting of traffic flows on the public PEMS-BAY dataset [45]. The traffic dataset is collected by California Transportation Agencies (CalTrans) Performance Measurement System (PeMS) from January 1st 2017 to May 31st 2017. We follow the same experimental setup as that in Li et al. [45]. The number of traffic sensors is 325. The traffic speed readings are aggregated into 5-min windows and the data are split by 70/10/20 into train/validation/test sets. The task is to predict the future 1 hour traffic flow (i.e., prediction horizon = 12 time steps) given the previous 1 hour traffic flow (12 time steps). The resolution r is set to be 12

¹SimpleSleepNet: <https://github.com/Dreem-Organization/dreem-learning-open>; RobustSleepNet: <https://github.com/Dreem-Organization/RobustSleepNet>

time steps. This is a transductive node-level forecasting task, therefore we adopt Equation 6 for graph structure learning. The traffic graph is directed.

We compare our model performance to existing traffic forecasting models: (1) DCRNN [45], (2) Graph WaveNet [71], (3) Graph Multi-Attention Network (GMAN) [78], (4) Traffic Transformer [9], (5) Spacetimeformer [28], and (6) Adaptive Graph Spatial-Temporal Transformer Network (ASTTN) [21]. DCRNN, Graph WaveNet, and GMAN are temporal GNNs, whereas the rest are Transformer-based models. Following previous works, we use mean absolute error (MAE), root mean squared error (RMSE), and mean absolute percentage error (MAPE) as the evaluation metrics.

5.2 Experimental results

Seizure detection from EEG signals. Table 1 shows our model performance on EEG-based seizure detection and its comparison to existing models. GRAPH4MER outperforms the previous state-of-the-art, Dist-DCRNN with pretraining, by 3.1 points in AUROC. Notably, Dist-DCRNN was pretrained using a self-supervised task [66], whereas GRAPH4MER was trained from scratch.

Table 1: **Results of EEG-based seizure detection on TUSZ dataset.** Baseline model results are cited from Tang et al. [66]. Best and second best results are **bolded** and underlined, respectively.

Model	AUROC
LSTM [34]	0.715 ± 0.016
Dense-CNN [59]	0.796 ± 0.014
CNN-LSTM [2]	0.682 ± 0.003
Dist-DCRNN w/o Pretraining [66]	0.793 ± 0.022
Corr-DCRNN w/o Pretraining [66]	0.804 ± 0.015
Dist-DCRNN w/ Pretraining [66]	<u>0.875 ± 0.016</u>
Corr-DCRNN w/ Pretraining [66]	0.850 ± 0.014
GRAPH4MER (ours)	0.906 ± 0.012

Sleep staging from PSG signals. Table 2 compares our model performance to existing sleep staging models on DOD-H dataset. GRAPH4MER outperforms RobustSleepNet, a specialized sleep staging model, by 4.1 points in macro-F1. It is important to note that both SimpleSleepNet and RobustSleepNet preprocess the PSG signals using short-time Fourier transform, whereas our model directly operates on raw PSG signals without the need of preprocessing.

Table 2: **Results of sleep staging on DOD-H dataset.** Best and second best results are **bolded** and underlined, respectively.

Model	Macro-F1	Kappa
LSTM [34]	0.609 ± 0.034	0.539 ± 0.046
SimpleSleepNet [33]	0.720 ± 0.001	0.703 ± 0.013
RobustSleepNet [32]	<u>0.777 ± 0.007</u>	<u>0.758 ± 0.008</u>
GRAPH4MER (ours)	0.818 ± 0.008	0.802 ± 0.014

Traffic forecasting. Table 3 shows the performance of our model and existing traffic forecasting models on PEMS-BAY. We observe that GRAPH4MER outperforms temporal GNNs (DCRNN, Graph WaveNet, GMAN) by a large margin and performs better than Transformer-based models (ASTTN and Spacetimeformer) in MAE.

Notably, the three tasks cover a wide range of sequence lengths ranging from 12 to 12k time steps. GRAPH4MER outperforms previous state-of-the-art on all of the three tasks, suggesting that it is capable of capturing long-range temporal dependencies across a wide range of sequence lengths.

Effect of GSL. As GSL is an important component of GRAPH4MER, we investigate the effect of GSL on the model performance. Table 4 shows the model performance when we remove the GSL layer in GRAPH4MER and use predefined graphs. For seizure detection on TUSZ dataset, we use the

Table 3: **Results of traffic forecasting on PEMS-BAY dataset.** Baseline model results are cited from the literature. Best and second best results are **bolded** and underlined, respectively.

Model	MAE	RMSE	MAPE
DCRNN [45]	2.07	4.74	4.90%
Graph WaveNet [71]	1.95	4.52	4.63%
GMAN [78]	1.86	4.32	4.31%
Traffic Transformer [9]	1.77	4.36	4.29%
Spacetimeformer [28]	1.73	3.79	3.85%
ASTTN [21]	<u>1.72</u>	4.02	3.98%
GRAPHS4MER (ours)	1.696 ± 0.008	<u>3.989 ± 0.023</u>	3.86% ± 0.02%

predefined distance-based EEG graph as in Tang et al. [66]; for traffic forecasting on PEMS-BAY, we use the predefined traffic sensor graph as in Li et al. [45]. DOD-H dataset has no predefined graph available, and thus we use a KNN graph obtained based on cosine similarity between nodes using S4 embeddings ($K = 3$; same as GRAPHS4MER). We observe that GRAPHS4MER using GSL outperforms GRAPHS4MER with predefined graph on the TUSZ and DOD-H datasets, but not on the PEMS-BAY dataset. This suggests that sensor locations used for constructing the predefined traffic sensor graph [45] are critical for traffic forecasting. Nevertheless, a major advantage of our GSL method is that it does not require prior knowledge about the graph structure, which would be particularly useful when sensor locations are not available.

Table 4: Comparison of predefined graphs vs GSL. Best results are **bolded**.

Model	TUSZ (AUROC)	DOD-H (Macro-F1)	PEMS-BAY (MAE)
GRAPHS4MER w/ predefined graph (w/o GSL)	0.899 ± 0.010	0.765 ± 0.016	1.629 ± 0.003
GRAPHS4MER (w/ GSL)	0.906 ± 0.012	0.818 ± 0.008	1.696 ± 0.008

Ablations. We perform ablation studies to investigate the importance of (1) graph-based representation, where we remove the GSL and GNN layers in our model and (2) S4 encoder, where we replace the S4 layers with GRUs [13]. Table 5 shows the ablation results. There are several important observations. First, GRAPHS4MER consistently outperforms S4, suggesting the effectiveness of representing multivariate signals as graphs. Second, when S4 layers are replaced with GRUs, the model performance drops by a large margin, particularly on TUH and DOD-H datasets with long sequences (12k and 7.5k time steps, respectively). This indicates the effectiveness of S4 in modeling long-term temporal dependencies.

Effect of temporal resolution. We examine the effect of temporal resolution r in Figure 3 in Appendix D. We observe that dynamically varying graph structures are more useful for inductive tasks (i.e., seizure detection and sleep staging) than the transductive traffic forecasting task.

Table 5: **Ablation results.** For S4, we remove the GSL and GNN layers. For GRAPHS4MER w/o S4, we replace S4 with GRUs. Best and second best results are **bolded** and underlined, respectively.

Model	TUSZ (AUROC)	DOD-H (Macro-F1)	PEMS-BAY (MAE)
S4	0.824 ± 0.011	0.778 ± 0.009	2.262 ± 0.004
GRAPHS4MER w/o S4	0.705 ± 0.095	0.634 ± 0.061	<u>1.723 ± 0.006</u>
GRAPHS4MER	0.906 ± 0.012	0.818 ± 0.008	1.696 ± 0.008

Visualization of graphs. To investigate if the learned graphs are interpretable, we visualize mean adjacency matrices for EEG and PSG signals in the correctly predicted test samples in Figure 2, grouped by seizure classes and sleep stages. For EEG, we observe that the differences between generalized seizure and non-seizure adjacency matrices (Figure 2e) are larger than the differences between focal seizure and non-seizure adjacency matrices (Figure 2d). This suggests that generalized seizures disrupt normal brain connectivity more than focal seizures, which is consistent with the literature that brain functional connectivity changes significantly in generalized seizures [64]. For

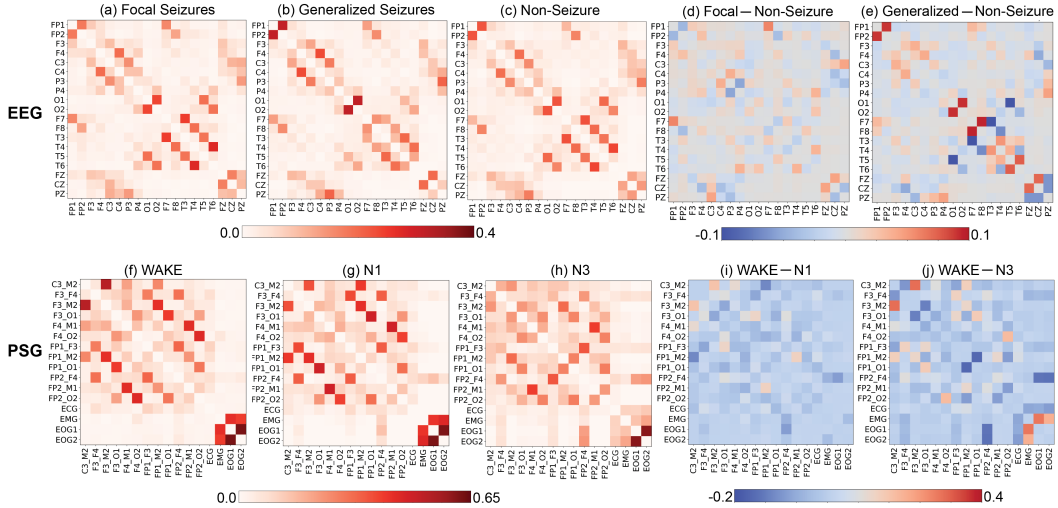


Figure 2: **Top**: Mean adjacency matrix for EEG in correctly predicted test samples for (a) focal seizures, (b) generalized seizures, and (c) non-seizure EEG clips. (d) Difference between focal seizure and non-seizure adjacency matrices. (e) Difference between generalized seizure and non-seizure adjacency matrices. **Bottom**: Mean adjacency matrix for PSG in correctly predicted test samples for sleep stage (f) WAKE, (g) N1, and (h) N3. (i) Difference between WAKE and N1 adjacency matrices. (j) Difference between WAKE and N3 adjacency matrices. Self-edges (i.e., diagonal) are not shown here.

PSG, we observe that the differences between N3 and wake (Figure 2j) are larger than the differences between N1 and wake (Figure 2i). This pattern is expected given that N1 is the earliest sleep stage, whereas N3 is the deep sleep stage and is associated with slow brain waves that are not present in other sleep stages [1]. Mean adjacency matrices for sleep stages N2 and REM are shown in Appendix E and Figure 4. In addition, we visualize the learned adjacency matrix for traffic forecasting in Appendix F and Figure 5. We also show example dynamic graphs for an EEG clip in Appendix G and Figure 6.

6 Conclusion and Future Work

In conclusion, we propose a novel graph structure learning method to learn dynamically evolving graph structures in multivariate signals, and present GRAPH-S4MER, a general GNN architecture integrating Structured State Spaces model and graph structure learning for spatiotemporal modeling of multivariate signals. Our method sets new state-of-the-art on seizure detection, sleep staging, and traffic forecasting, and learns meaningful graph structures that reflect seizure classes and sleep stages. Importantly, our method does not require prior knowledge about the graph structure, and thus would be particularly useful for applications where graph structures cannot be easily predefined. Our study opens exciting future directions for graph-based spatiotemporal modeling of multivariate signals, including (1) leveraging domain knowledge for improved graph structure learning, (2) investigating other ways of combining S4 and GSL to further improve long-range graph structure learning, and (3) applying to other types of time series.

Acknowledgments

We thank HAI and Google Cloud for the support of Google Cloud credits for this work.

References

- [1] Academy Sleep Medicine. The AASM manual for the scoring of sleep and associated events: rules, terminology and technical specifications. , *IL: American Academy of Sleep Medicine*, 2007.

- [2] David Ahmedt-Aristizabal, Tharindu Fernando, Simon Denman, Lars Petersson, Matthew J Aburn, and Clinton Fookes. Neural memory networks for seizure type classification. *Conf. Proc. IEEE Eng. Med. Biol. Soc.*, 2020:569–575, July 2020.
- [3] Martin Arjovsky, Amar Shah, and Yoshua Bengio. Unitary evolution recurrent neural networks. In Maria Florina Balcan and Kilian Q Weinberger, editors, *Proceedings of The 33rd International Conference on Machine Learning*, volume 48 of *Proceedings of Machine Learning Research*, pages 1120–1128, New York, New York, USA, 2016.
- [4] Umar Asif, Subhrajit Roy, Jianbin Tang, and Stefan Harrer. SeizureNet: Multi-Spectral deep feature learning for seizure type classification. In *Machine Learning in Clinical Neuroimaging and Radiogenomics in Neuro-oncology*, pages 77–87. Springer International Publishing, 2020.
- [5] LEI Bai, Lina Yao, Can Li, Xianzhi Wang, and Can Wang. Adaptive graph convolutional recurrent network for traffic forecasting. In H Larochelle, M Ranzato, R Hadsell, M F Balcan, and H Lin, editors, *Advances in Neural Information Processing Systems*, volume 33, pages 17804–17815. Curran Associates, Inc., 2020.
- [6] Belkin and Niyogi. Laplacian eigenmaps and spectral techniques for embedding and clustering. *Adv. Neural Inf. Process. Syst.*, 2001.
- [7] Luc Berthouze, Leon M James, and Simon F Farmer. Human EEG shows long-range temporal correlations of oscillation amplitude in theta, alpha and beta bands across a wide age range. *Clin. Neurophysiol.*, 121(8):1187–1197, August 2010.
- [8] Michael M Bronstein, Joan Bruna, Yann LeCun, Arthur Szlam, and Pierre Vandergheynst. Geometric deep learning: Going beyond euclidean data. *IEEE Signal Process. Mag.*, 34(4):18–42, July 2017.
- [9] Ling Cai, Krzysztof Janowicz, Gengchen Mai, Bo Yan, and Rui Zhu. Traffic transformer: Capturing the continuity and periodicity of time series for traffic forecasting. *Trans. GIS*, 24(3):736–755, June 2020.
- [10] Enrico Camporeale, Simon Wing, and Jay Johnson. *Machine Learning Techniques for Space Weather*. Elsevier, May 2018.
- [11] Chami, Abu-El-Haija, Perozzi, Ré, and others. Machine learning on graphs: A model and comprehensive taxonomy. *Journal of Machine Learning Research*, 2022.
- [12] Yu Chen, Lingfei Wu, and Mohammed Zaki. Iterative deep graph learning for graph neural networks: Better and robust node embeddings. *Adv. Neural Inf. Process. Syst.*, 33:19314–19326, 2020.
- [13] Kyunghyun Cho, Bart van Merriënboer, Dzmitry Bahdanau, and Yoshua Bengio. On the properties of neural machine translation: Encoder-Decoder approaches. September 2014.
- [14] Krzysztof Marcin Choromanski, Valerii Likhoshesterov, David Dohan, Xingyou Song, Andreea Gane, Tamas Sarlos, Peter Hawkins, Jared Quincy Davis, Afroz Mohiuddin, Lukasz Kaiser, David Benjamin Belanger, Lucy J Colwell, and Adrian Weller. Rethinking attention with performers. In *International Conference on Learning Representations*, 2021. URL <https://openreview.net/forum?id=Ua6zuk0WRH>.
- [15] Ian C Covert, Balu Krishnan, Imad Najm, Jiening Zhan, Matthew Shore, John Hixson, and Ming Jack Po. Temporal graph convolutional networks for automatic seizure detection. In Finale Doshi-Velez, Jim Fackler, Ken Jung, David Kale, Rajesh Ranganath, Byron Wallace, and Jenna Wiens, editors, *Proceedings of the 4th Machine Learning for Healthcare Conference*, volume 106 of *Proceedings of Machine Learning Research*, pages 160–180. PMLR, 2019.
- [16] da Xu, chuanwei ruan, evren korpeoglu, sushant kumar, and kannan achan. Inductive representation learning on temporal graphs. In *International Conference on Learning Representations*, 2020. URL <https://openreview.net/forum?id=rJeW1yHYwH>.

- [17] Defferrard, Bresson, and others. Convolutional neural networks on graphs with fast localized spectral filtering. *Adv. Neural Inf. Process. Syst.*, 2016.
- [18] Ahmed El-Gazzar, Rajat Mani Thomas, and Guido van Wingen. Dynamic adaptive Spatio-Temporal graph convolution for fMRI modelling. In Ahmed Abdulkadir, Seyed Mostafa Kia, Mohamad Habes, Vinod Kumar, Jane Maryam Rondina, Chantal Tax, and Thomas Wolfers, editors, *Machine Learning in Clinical Neuroimaging*, pages 125–134, Cham, 2021. Springer International Publishing.
- [19] N. Benjamin Erichson, Omri Azencot, Alejandro Queiruga, Liam Hodgkinson, and Michael W. Mahoney. Lipschitz recurrent neural networks. In *International Conference on Learning Representations*, 2021. URL <https://openreview.net/forum?id=-N7PBXqOUJZ>.
- [20] Alireza Ermagun and David Levinson. Spatiotemporal traffic forecasting: review and proposed directions. *Transp. Rev.*, 38(6):786–814, November 2018.
- [21] Aosong Feng and Leandros Tassioulas. Adaptive graph Spatial-Temporal transformer network for traffic flow forecasting. July 2022.
- [22] Tianfan Fu, Wenhao Gao, Cao Xiao, Jacob Yasonik, Connor W. Coley, and Jimeng Sun. Differentiable scaffolding tree for molecular optimization, 2021. URL <https://arxiv.org/abs/2109.10469>.
- [23] Jianfei Gao and Bruno Ribeiro. On the equivalence between temporal and static equivariant graph representations. In Kamalika Chaudhuri, Stefanie Jegelka, Le Song, Csaba Szepesvari, Gang Niu, and Sivan Sabato, editors, *Proceedings of the 39th International Conference on Machine Learning*, volume 162 of *Proceedings of Machine Learning Research*, pages 7052–7076. PMLR, 2022.
- [24] Xiang Gao, Wei Hu, and Zongming Guo. Exploring Structure-Adaptive graph learning for robust Semi-Supervised classification. In *2020 IEEE International Conference on Multimedia and Expo (ICME)*, pages 1–6. ieeexplore.ieee.org, July 2020.
- [25] Ahmed El Gazzar, Rajat Mani Thomas, and Guido Van Wingen. Improving the diagnosis of psychiatric disorders with self-supervised graph state space models, 2022. URL <https://arxiv.org/abs/2206.03331>.
- [26] Ahmed El Gazzar, Rajat Mani Thomas, and Guido Van Wingen. Improving the diagnosis of psychiatric disorders with self-supervised graph state space models, 2022. URL <https://arxiv.org/abs/2206.03331>.
- [27] Karan Goel, Albert Gu, Chris Donahue, and Christopher Re. It’s raw! Audio generation with state-space models. In Kamalika Chaudhuri, Stefanie Jegelka, Le Song, Csaba Szepesvari, Gang Niu, and Sivan Sabato, editors, *Proceedings of the 39th International Conference on Machine Learning*, volume 162 of *Proceedings of Machine Learning Research*, pages 7616–7633. PMLR, 17–23 Jul 2022. URL <https://proceedings.mlr.press/v162/goe122a.html>.
- [28] Jake Grigsby, Zhe Wang, and Yanjun Qi. Long-range transformers for dynamic spatiotemporal forecasting, 2022. URL <https://arxiv.org/abs/2109.12218>.
- [29] Gu, Dao, Ermon, Rudra, and others. Hippo: Recurrent memory with optimal polynomial projections. *Adv. Neural Inf. Process. Syst.*, 2020.
- [30] Gu, Johnson, Goel, Saab, and others. Combining recurrent, convolutional, and continuous-time models with linear state space layers. *Adv. Neural Inf. Process. Syst.*, 2021.
- [31] Albert Gu, Karan Goel, and Christopher Re. Efficiently modeling long sequences with structured state spaces. In *International Conference on Learning Representations*, 2022.
- [32] Antoine Guillot and Valentin Thorey. RobustSleepNet: Transfer learning for automated sleep staging at scale. *IEEE Trans. Neural Syst. Rehabil. Eng.*, 29:1441–1451, July 2021.

- [33] Antoine Guillot, Fabien Sauvet, Emmanuel H During, and Valentin Thorey. Dreem open datasets: Multi-Scored sleep datasets to compare human and automated sleep staging. *IEEE Trans. Neural Syst. Rehabil. Eng.*, 28(9):1955–1965, September 2020.
- [34] S Hochreiter and J Schmidhuber. Long short-term memory. *Neural Comput.*, 9(8):1735–1780, November 1997.
- [35] Weihua Hu, Bowen Liu, Joseph Gomes, Marinka Zitnik, Percy Liang, Vijay Pande, and Jure Leskovec. Strategies for pre-training graph neural networks. In *International Conference on Learning Representations*, 2020. URL <https://openreview.net/forum?id=HJ1WWJSFDH>.
- [36] H H Jasper. The ten-twenty electrode system of the international federation. *Electroencephalogr. Clin. Neurophysiol.*, 10:370–375, 1958.
- [37] Ziyu Jia, Youfang Lin, Jing Wang, Ronghao Zhou, Xiaojun Ning, Yuanlai He, and Yaoshuai Zhao. Graphsleepnet: Adaptive spatial-temporal graph convolutional networks for sleep stage classification. In Christian Bessiere, editor, *Proceedings of the Twenty-Ninth International Joint Conference on Artificial Intelligence, IJCAI-20*, pages 1324–1330. International Joint Conferences on Artificial Intelligence Organization, 7 2020. doi: 10.24963/ijcai.2020/184. URL <https://doi.org/10.24963/ijcai.2020/184>. Main track.
- [38] Weiwei Jiang and Jiayun Luo. Graph neural network for traffic forecasting: A survey. *Expert Syst. Appl.*, 207:117921, November 2022.
- [39] Wei Jin, Yao Ma, Xiaorui Liu, Xianfeng Tang, Suhang Wang, and Jiliang Tang. Graph structure learning for robust graph neural networks. In *Proceedings of the 26th ACM SIGKDD International Conference on Knowledge Discovery and Data Mining, KDD '20*, page 66–74, New York, NY, USA, 2020. Association for Computing Machinery. ISBN 9781450379984. doi: 10.1145/3394486.3403049. URL <https://doi.org/10.1145/3394486.3403049>.
- [40] Vassilis Kalofolias. How to learn a graph from smooth signals. In *Proceedings of the 19th International Conference on Artificial Intelligence and Statistics*, volume 51 of *Proceedings of Machine Learning Research*, pages 920–929, Cadiz, Spain, 2016. PMLR.
- [41] Amol Kapoor, Xue Ben, Luyang Liu, Bryan Perozzi, Matt Barnes, Martin Blais, and Shawn O’Banion. Examining covid-19 forecasting using spatio-temporal graph neural networks, 2020. URL <https://arxiv.org/abs/2007.03113>.
- [42] Katharopoulos, Vyas, Pappas, and others. Transformers are rnns: Fast autoregressive transformers with linear attention. *on Machine Learning*, 2020.
- [43] Jia Li, Zhichao Han, Hong Cheng, Jiao Su, Pengyun Wang, Jianfeng Zhang, and Lujia Pan. Predicting path failure in Time-Evolving graphs. In *Proceedings of the 25th ACM SIGKDD International Conference on Knowledge Discovery & Data Mining, KDD '19*, pages 1279–1289, New York, NY, USA, July 2019. Association for Computing Machinery.
- [44] Ruoyu Li, Sheng Wang, Feiyun Zhu, and Junzhou Huang. Adaptive graph convolutional neural networks. *AAAI*, 32(1), April 2018.
- [45] Yaguang Li, Rose Yu, Cyrus Shahabi, and Yan Liu. Diffusion convolutional recurrent neural network: Data-driven traffic forecasting. In *International Conference on Learning Representations*, 2018. URL <https://openreview.net/forum?id=SJiHXGWAZ>.
- [46] Ilya Loshchilov and Frank Hutter. SGDR: Stochastic gradient descent with warm restarts. In *International Conference on Learning Representations*, 2017. URL <https://openreview.net/forum?id=Skq89Scxx>.
- [47] Ilya Loshchilov and Frank Hutter. Decoupled weight decay regularization. In *International Conference on Learning Representations*, 2019. URL <https://openreview.net/forum?id=Bkg6RiCqY7>.

- [48] Dongsheng Luo, Wei Cheng, Wenchao Yu, Bo Zong, Jingchao Ni, Haifeng Chen, and Xiang Zhang. Learning to drop: Robust graph neural network via topological denoising. In *Proceedings of the 14th ACM International Conference on Web Search and Data Mining, WSDM '21*, pages 779–787, New York, NY, USA, March 2021. Association for Computing Machinery.
- [49] Christoph M Michel and Micah M Murray. Towards the utilization of EEG as a brain imaging tool. *Neuroimage*, 61(2):371–385, June 2012.
- [50] Ana Mincholé, Julià Camps, Aurore Lyon, and Blanca Rodríguez. Machine learning in the electrocardiogram. *J. Electrocardiol.*, 57S:S61–S64, November 2019.
- [51] Michael Negnevitsky, Paras Mandal, and Anurag K Srivastava. Machine learning applications for load, price and wind power prediction in power systems. In *2009 15th International Conference on Intelligent System Applications to Power Systems*, pages 1–6. ieeexplore.ieee.org, November 2009.
- [52] Antonio Ortega, Pascal Frossard, Jelena Kovačević, José M F Moura, and Pierre Vandergheynst. Graph signal processing: Overview, challenges, and applications. *Proc. IEEE*, 106(5):808–828, May 2018.
- [53] George Panagopoulos, Giannis Nikolentzos, and Michalis Vazirgiannis. Transfer graph neural networks for pandemic forecasting. *AAAI*, 35(6):4838–4845, May 2021.
- [54] Aldo Pareja, Giacomo Domeniconi, Jie Chen, Tengfei Ma, Toyotaro Suzumura, Hiroki Kanezashi, Tim Kaler, Tao Schardl, and Charles Leiserson. EvolveGCN: Evolving graph convolutional networks for dynamic graphs. *AAAI*, 34(04):5363–5370, April 2020.
- [55] Huy Phan and Kaare Mikkelsen. Automatic sleep staging of EEG signals: recent development, challenges, and future directions. *Physiol. Meas.*, 43(4), April 2022.
- [56] Ashirbad Pradhan, Jiayuan He, and Ning Jiang. Hand gesture recognition and biometric authentication using a multi-day dataset. In *Intelligent Robotics and Applications*, pages 375–385. Springer International Publishing, 2022.
- [57] Ilene M Rosen, Douglas B Kirsch, Kelly A Carden, Raman K Malhotra, Kannan Ramar, R Nisha Aurora, David A Kristo, Jennifer L Martin, Eric J Olson, Carol L Rosen, James A Rowley, Anita V Shelgikar, and American Academy of Sleep Medicine Board of Directors. Clinical use of a home sleep apnea test: An updated american academy of sleep medicine position statement. *J. Clin. Sleep Med.*, 14(12):2075–2077, December 2018.
- [58] Emanuele Rossi, Ben Chamberlain, Fabrizio Frasca, Davide Eynard, Federico Monti, and Michael Bronstein. Temporal graph networks for deep learning on dynamic graphs, 2020. URL <https://arxiv.org/abs/2006.10637>.
- [59] Khaled Saab, Jared Dunnmon, Christopher Ré, Daniel Rubin, and Christopher Lee-Messer. Weak supervision as an efficient approach for automated seizure detection in electroencephalography. *NPJ Digit Med*, 3:59, April 2020.
- [60] Youngjoo Seo, Michaël Defferrard, Pierre Vandergheynst, and Xavier Bresson. Structured sequence modeling with graph convolutional recurrent networks. In *Neural Information Processing*, pages 362–373. Springer International Publishing, 2018.
- [61] Vinit Shah, Eva von Weltin, Silvia Lopez, James Riley McHugh, Lillian Veloso, Meysam Golmohammadi, Iyad Obeid, and Joseph Picone. The temple university hospital seizure detection corpus. *Front. Neuroinform.*, 12:83, November 2018.
- [62] Chao Shang, Jie Chen, and Jinbo Bi. Discrete graph structure learning for forecasting multiple time series. In *International Conference on Learning Representations*, 2021. URL <https://openreview.net/forum?id=WEHS1H5m0k>.

- [63] Afshin Shoeibi, Marjane Khodatars, Navid Ghassemi, Mahboobeh Jafari, Parisa Moridian, Roohallah Alizadehsani, Maryam Panahiazar, Fahime Khozeimeh, Assef Zare, Hossein Hosseini-Nejad, Abbas Khosravi, Amir F Atiya, Diba Aminshahidi, Sadiq Hussain, Modjtaba Rouhani, Saeid Nahavandi, and Udyavara Rajendra Acharya. Epileptic seizures detection using deep learning techniques: A review. *Int. J. Environ. Res. Public Health*, 18(11), May 2021.
- [64] Jintao Sun, Yihan Li, Ke Zhang, Yulei Sun, Yingfan Wang, Ailiang Miao, Jing Xiang, and Xiaoshan Wang. Frequency-Dependent dynamics of functional connectivity networks during seizure termination in childhood absence epilepsy: A magnetoencephalography study. *Front. Neurol.*, 12, 2021.
- [65] Jiabin Tang, Tang Qian, Shijing Liu, Shengdong Du, Jie Hu, and Tianrui Li. Spatio-temporal latent graph structure learning for traffic forecasting, 2022. URL <https://arxiv.org/abs/2202.12586>.
- [66] Siyi Tang, Jared Dunnmon, Khaled Kamal Saab, Xuan Zhang, Qianying Huang, Florian Dubost, Daniel Rubin, and Christopher Lee-Messer. Self-Supervised graph neural networks for improved electroencephalographic seizure analysis. In *International Conference on Learning Representations*, April 2022.
- [67] Yi Tay, Mostafa Dehghani, Samira Abnar, Yikang Shen, Dara Bahri, Philip Pham, Jinfeng Rao, Liu Yang, Sebastian Ruder, and Donald Metzler. Long range arena: A benchmark for efficient transformers, 2020. URL <https://arxiv.org/abs/2011.04006>.
- [68] Chenyu Tian and Wai Kin (victor) Chan. Spatial-temporal attention wavenet: A deep learning framework for traffic prediction considering spatial-temporal dependencies. *IET Intel. Transport Syst.*, 15(4):549–561, April 2021.
- [69] Vaswani, Shazeer, Parmar, and others. Attention is all you need. *Adv. Neural Inf. Process. Syst.*, 2017.
- [70] Yue Wang, Yongbin Sun, Ziwei Liu, Sanjay E Sarma, Michael M Bronstein, and Justin M Solomon. Dynamic graph CNN for learning on point clouds. *ACM Trans. Graph.*, 38(5):1–12, October 2019.
- [71] Zonghan Wu, Shirui Pan, Guodong Long, Jing Jiang, and Chengqi Zhang. Graph wavenet for deep spatial-temporal graph modeling. In *Proceedings of the Twenty-Eighth International Joint Conference on Artificial Intelligence, IJCAI-19*, pages 1907–1913. International Joint Conferences on Artificial Intelligence Organization, 7 2019. doi: 10.24963/ijcai.2019/264. URL <https://doi.org/10.24963/ijcai.2019/264>.
- [72] Keyulu Xu, Weihua Hu, Jure Leskovec, and Stefanie Jegelka. How powerful are graph neural networks? In *International Conference on Learning Representations*, 2019. URL <https://openreview.net/forum?id=ryGs6iA5Km>.
- [73] Weizhi Xu, Junfei Wu, Qiang Liu, Shu Wu, and Liang Wang. Evidence-aware fake news detection with graph neural networks. January 2022.
- [74] Qi Zhang, Jianlong Chang, Gaofeng Meng, Shiming Xiang, and Chunhong Pan. Spatio-Temporal graph structure learning for traffic forecasting. *AAAI*, 34(01):1177–1185, April 2020.
- [75] Xiang Zhang and Marinka Zitnik. GNNGuard: Defending graph neural networks against adversarial attacks. *Adv. Neural Inf. Process. Syst.*, 33:9263–9275, 2020.
- [76] Xiang Zhang, Marko Zeman, Theodoros Tsiligkaridis, and Marinka Zitnik. Graph-guided network for irregularly sampled multivariate time series. In *International Conference on Learning Representations*, 2022. URL <https://openreview.net/forum?id=Kwm8I7dU-15>.
- [77] Cheng Zheng, Bo Zong, Wei Cheng, Dongjin Song, Jingchao Ni, Wenchao Yu, Haifeng Chen, and Wei Wang. Robust graph representation learning via neural sparsification. In Hal Daumé III and Aarti Singh, editors, *Proceedings of the 37th International Conference on Machine Learning*, volume 119 of *Proceedings of Machine Learning Research*, pages 11458–11468. PMLR, 2020.

- [78] Chuanpan Zheng, Xiaoliang Fan, Cheng Wang, and Jianzhong Qi. GMAN: A graph Multi-Attention network for traffic prediction. *AAAI*, 34(01):1234–1241, April 2020.
- [79] Yanqiao Zhu, Weizhi Xu, Jinghao Zhang, Yuanqi Du, Jieyu Zhang, Qiang Liu, Carl Yang, and Shu Wu. A survey on graph structure learning: Progress and opportunities. March 2021.

Appendix

A Pseudocode for GraphS4mer

Algorithm 1 shows the pseudocode for GraphS4mer. Note that $n_d = \frac{T}{r}$ is the number of dynamic graphs, where T is the sequence length and r is the pre-specified resolution. While there is a for loop over $t = 1, \dots, n_d$, the code implementation can be done in batches to eliminate the need of a for loop.

Algorithm 1: Pseudocode for GraphS4mer.

```
Input : multivariate signal  $\mathbf{X}$ , label  $\mathbf{y}$ 
Parameter: model weights  $\theta$ , including weights for S4, GSL, GNN, and linear layers
Output : prediction  $\hat{\mathbf{y}}$ , learned graph adjacency matrices  $\mathbf{W}^{(1)}, \dots, \mathbf{W}^{(n_d)}$ 
1 Randomly initialize model weights  $\theta$ 
2 while not converged do
3    $\mathcal{L}_{\text{reg}} \leftarrow 0$ 
4   // step 1. get S4 embeddings
5    $\mathbf{H} \leftarrow \text{S4}(\mathbf{X})$ 
6   for  $t = 1, 2, \dots, n_d$  do
7      $\mathbf{h}^{(t)} \leftarrow \text{mean-pool}(\mathbf{H}_{:,((t-1) \times r):(t \times r),:})$  // mean-pool along temporal dim
8     // step 2. graph structure learning (GSL)
9     Construct KNN graph,  $\mathbf{W}_{\text{KNN}}^{(t)}$ , based on cosine similarity between nodes using  $\mathbf{h}^{(t)}$ 
10    if inductive setting then
11       $\mathbf{W}^{(t)} \leftarrow \text{GSL}(\mathbf{h}^{(t)}, \mathbf{W}_{\text{KNN}}^{(t)})$  using Eqn. 5 and Eqn. 7 // GSL in inductive
12      setting
13    else
14       $\mathbf{W}^{(t)} \leftarrow \text{GSL}(\mathbf{W}_{\text{KNN}}^{(t)})$  using Eqn. 6 and Eqn. 7 // GSL in transductive setting
15    end if
16     $\mathcal{L}_{\text{reg}} \leftarrow \mathcal{L}_{\text{reg}} + \alpha \mathcal{L}_{\text{smooth}}(\mathbf{h}^{(t)}, \mathbf{W}^{(t)}) + \beta \mathcal{L}_{\text{degree}}(\mathbf{W}^{(t)}) + \gamma \mathcal{L}_{\text{sparse}}(\mathbf{W}^{(t)})$  using Eqn. 3–4
17    // graph regularization loss
18    // step 3. get node embeddings from GNN
19    if graph classification task then
20       $\mathbf{z}^{(t)} \leftarrow \text{GNN}(\mathbf{h}^{(t)}, \mathbf{W}^{(t)})$  //  $\mathbf{z}^{(t)}$  has shape  $(N, 1, D_{\text{hidden}})$ 
21    else
22       $\mathbf{z}^{(t)} \leftarrow \text{GNN}(\mathbf{H}_{:,((t-1) \times r):(t \times r),:}, \mathbf{W}^{(t)})$  //  $\mathbf{z}^{(t)}$  has shape  $(N, r, D_{\text{hidden}})$ 
23    end if
24     $\mathbf{Z} \leftarrow \text{concat}(\mathbf{z}^{(1)}, \mathbf{z}^{(2)}, \dots, \mathbf{z}^{(n_d)})$  // concatenate along temporal dim
25    // step 4. pooling and fully connected layers
26    if graph classification task then
27       $\mathbf{Z} \leftarrow \text{graph-pool}(\text{temporal-pool}(\mathbf{Z}))$ 
28       $\hat{\mathbf{y}} \leftarrow \text{Linear}(\mathbf{Z})$ 
29       $\mathcal{L}_{\text{pred}} \leftarrow \mathcal{L}_{\text{cross-entropy}}(\hat{\mathbf{y}}, \mathbf{y})$  // loss for classification
30    else
31       $\hat{\mathbf{y}} \leftarrow \text{Linear}(\mathbf{Z})$ 
32       $\mathcal{L}_{\text{pred}} \leftarrow \mathcal{L}_{\text{MAE}}(\hat{\mathbf{y}}, \mathbf{y})$  // loss for forecasting
33    end if
34     $\mathcal{L} \leftarrow \mathcal{L}_{\text{pred}} + \frac{1}{n_d} \mathcal{L}_{\text{reg}}$  // total loss
35    Back-propagate  $\mathcal{L}$  to update model weights  $\theta$ 
36 end while
```

B Details of datasets

Temple University Hospital Seizure Detection Corpus (TUSZ). We use the publicly available Temporal University Hospital Seizure Detection Corpus (TUSZ) v1.5.2. for seizure detection [61]. We

follow the same experimental setup as in Tang et al. [66]. The TUSZ train set is divided into train and validation splits with distinct patients, and the TUSZ test set is held-out for model evaluation. The following 19 EEG channels are included: FP1, FP2, F3, F4, C3, C4, P3, P4, O1, O2, F7, F8, T3, T4, T5, T6, FZ, CZ, and PZ. Because the EEG signals are sampled at different sampling rate, we resample all the EEG signals to 200 Hz. Following a prior study [66], we also exclude 5 patients in the TUSZ test set who appear in both the TUSZ train and test sets. The EEG signals are divided into 60-s EEG clips without overlaps, and the task is to predict whether or not an EEG clip contains seizure. Table 6 shows the number of EEG clips and patients in the train, validation, and test splits.

Table 6: Number of EEG clips and patients in train, validation, and test splits of TUSZ dataset.

Train Set		Validation Set		Test Set	
EEG Clips (% Seizure)	Patients (% Seizure)	EEG Clips (% Seizure)	Patients (% Seizure)	EEG Clips (% Seizure)	Patients (% Seizure)
38,613 (9.3%)	530 (34.0%)	5,503 (11.4%)	61 (36.1%)	8,848 (14.7%)	45 (77.8%)

Dreem Open Dataset-Healthy (DOD-H). We use the publicly available Dreem Open Dataset-Healthy (DOD-H) for sleep staging [33]. The DOD-H dataset consists of overnight PSG sleep recordings from 25 volunteers. The PSG signals are measured from 12 EEG channels, 1 electromyographic (EMG) channel, 2 electrooculography (EOG) channels, and 1 electrocardiogram channel using a Siesta PSG device (Compumedics). All the signals are sampled at 250 Hz. Following the standard AASM Scoring Manual and Recommendations [57], each 30-s PSG signal is annotated by a consensus of 5 experienced sleep technologists as one of the five sleep stages: wake (W), rapid eye movement (REM), non-REM sleep stages N1, N2, and N3. We randomly split the PSG signals by 60/20/20 into train/validation/test splits, where each split has distinct subjects. Table 7 shows the number of 30-s PSG clips, the number of subjects, and the five sleep stage distributions.

Table 7: Number of subjects and 30-s PSG clips in the train, validation, and test splits of DOD-H dataset.

	Subjects	30-s PSG Clips					
		Total	Wake	N1	N2	N3	REM
Train Set	15	14,823	1,839	925	6,965	2,015	3,079
Validation Set	5	5,114	480	254	2,480	990	910
Test Set	5	4,725	718	326	2,434	509	738

PEMS-BAY traffic dataset. The PEMS-BAY dataset is collected by California Transportation Agencies (CalTrans) Performance Measurement System (PeMS). We follow the same experimental setup as in Li et al. [45]. Specifically, 325 sensors in the Bay Area are selected with 6 months of data ranging from January 1st to May 31st, 2017. The traffic speed readings are aggregated into 5-min windows. The total number of observed traffic data points is 16,937,179. 70% of the data are used for training, 20% are used for testing, and the remaining 10% are used for validation.

C Details of model training procedures and hyperparameters

Model training was accomplished using the AdamW optimizer [47] in PyTorch on a single NVIDIA A100 GPU. All experiments were run for three runs with different random seeds. Cosine learning rate scheduler with 5-epoch warm start was used [46]. Model training was early stopped when the validation loss did not decrease for 20 consecutive epochs. We performed the following hyperparameter search on the validation set: (1) initial learning rate within range [1e-4, 1e-2]; (2) dropout rate in S4 and GNN layers within range [0.1, 0.5]; (3) hidden dimension of S4 and GNN layers within range {64, 128, 256}; (4) number of S4 layers within range {2, 3, 4}; (5) S4 bidirectionality; (6) number of GNN layers within range {1, 2}; (7) graph pooling within range {mean-pool, max-pool, sum-pool} (only for graph classification tasks); (8) value of κ threshold for graph pruning by keeping the top $\kappa\%$ edges (within range {1, 2, 3, 4, 5, 6, 7, 8, 9, 10}) or keeping edges whose weights $> \kappa$ (within range {0.1, 0.2, 0.3, 0.4, 0.5}); (9) KNN graph with $K \in \{2, 3\}$; (10) weight of KNN graph $\epsilon \in [0.3, 0.6]$; (11) α, β ,

and γ weights in graph regularization within range $[0, 1]$; (12) learnable embedding ($\mathbf{E}^{(t)}$ in Equation 6) dimension within range $\{10, 12, 16\}$ (only for traffic forecasting).

Model training and hyperparameters for seizure detection on TUSZ dataset. As there are many more negative samples in the dataset, we undersampled the negative examples in the train set during training. We used binary cross-entropy loss as the loss function. The models were trained for 100 epochs with an initial learning rate of $8e-4$. The batch size was 4; dropout rate was 0.1; hidden dimension was 128; number of stacked S4 layers was 4; S4 layers were unidirectional; number of GNN layers was 1; graph pooling was max-pool and temporal pooling was mean-pool; graph pruning was done by setting a threshold of 0.1, where edges whose edge weights ≤ 0.1 were removed; $K = 2$ for KNN graph and the KNN graph weight ϵ was 0.6; α , β , and γ weights were all set to 0.05. This results in 265k trainable parameters in GRAPH4MER. Best model was picked based on the highest AUROC on the validation set.

Model training and hyperparameters for sleep staging on DOD-H dataset. As the DOD-H dataset is highly imbalanced, we undersampled the majority classes in the train set during training. We used cross-entropy loss as the loss function. The models were trained for 100 epochs with an initial learning rate of $1e-3$. The batch size was 4; dropout rate was 0.4; hidden dimension was 128; number of stacked S4 layers was 4 and S4 layers were unidirectional; number of GNN layers was 1; graph pooling was sum-pool and temporal pooling was mean-pool; graph pruning was done by setting a threshold of 0.1; $K = 3$ for KNN graph and the weight for KNN graph ϵ was 0.6; α , β , and γ weights were all set to 0.2. This results in 266k trainable parameters in GRAPH4MER. Best model was picked based on the highest macro-F1 score on the validation set.

Model training and hyperparameters for traffic forecasting on PEMS-BAY. Following Li et al. [45], we used mean absolute error (MAE) as the loss function. The models were trained for 100 epochs with an initial learning rate of $1e-3$. The batch size was 32; dropout rate was 0.1; hidden dimension was 256; number of stacked S4 layers was 4 and S4 layers were bidirectional; number of GNN layers was 2; graph pruning was done by keeping the top 2% edges in the graph; $K = 3$ for KNN graph and the weight for KNN graph ϵ was 0.5; α , β , and γ weights were 0.1, 0.2, and 0.2, respectively; the learnable embedding dimension was 16. This results in 865k trainable parameters in GRAPH4MER. Best model was picked based on the lowest MAE on the validation set.

D Effect of temporal resolution

To examine the effect of temporal resolution r on model performance, we show the performance versus different values of r in Figure 3. We observe that for inductive tasks (i.e., seizure detection and sleep staging), smaller value of r tends to result in higher performance, which suggests that capturing dynamically varying graph structures is useful for inductive tasks. In contrast, for transductive traffic forecasting task, larger value of r tends to give better performance, which suggests that learning a static graph is sufficient for the traffic forecasting task.

E Visualization of PSG graphs for five sleep stages

Figure 4 shows mean adjacency matrices for PSG signals in correctly predicted test samples grouped by five sleep stages. We observe that N3 differs from wake stage more than N1 (also see Figure 2). Moreover, in REM stage, the EMG channel has very weak connection to all other channels, which is expected given that one experiences muscle paralysis in REM stage.

F Visualization of traffic sensor graph

Figure 5 shows the mean adjacency matrix for traffic forecasting on PEMS-BAY dataset inferred by our GSL layer, as well as the adjacency matrix in Li et al. [45] predefined by sensor locations. The learned adjacency matrix (Figure 5a) does not exhibit block structures as in the predefined adjacency matrix (Figure 5b), which could be the reason why learning the traffic sensor graph results in lower performance than the predefined sensor graph (Table 4). This also suggests that future work should explore integrating prior knowledge of the graph in the GSL layer.

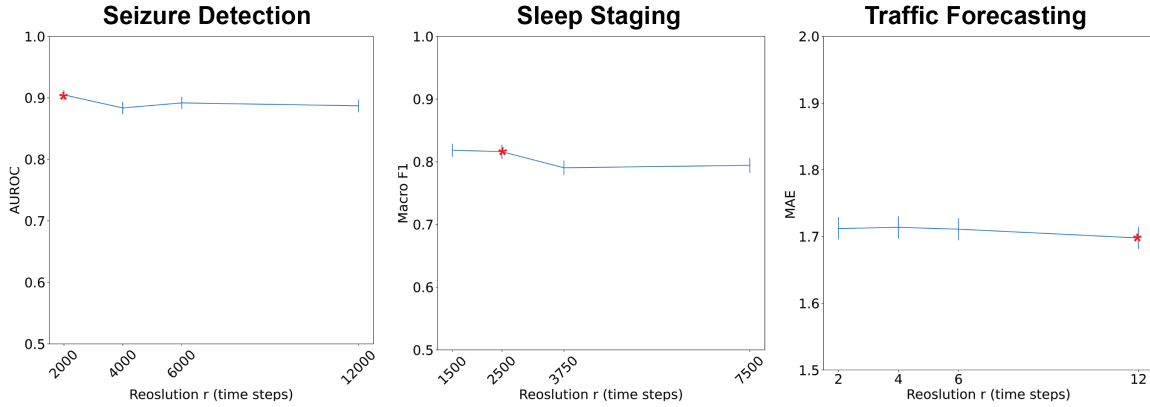


Figure 3: Model performance versus temporal resolution using the run with median performance. For convenience, we assume that temporal resolution is chosen so that the sequence length is divisible by the resolution. Asterisk indicates the temporal resolution used to report results for GRAPHS4MER in Table 1–5. Error bars indicate 95% confidence intervals obtained using bootstrapping with 5,000 replicates with replacement.

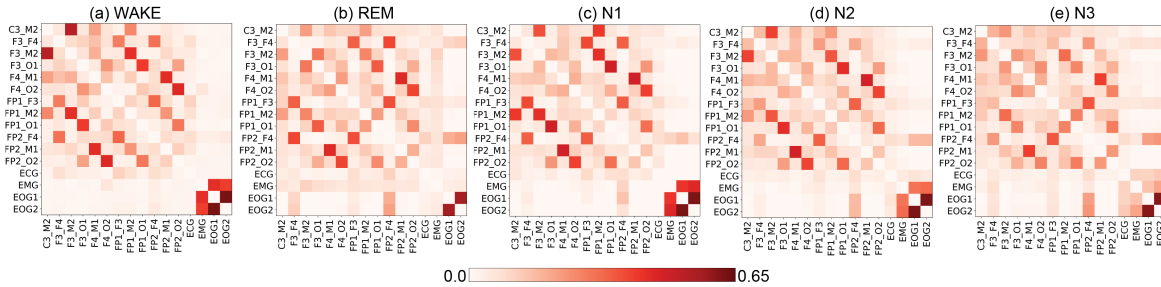


Figure 4: Mean adjacency matrix for PSG signals for five sleep stages in correctly predicted test samples. Self-edges (i.e., diagonal) are not shown here.

G Visualization of dynamic EEG graphs

In Figure 6, we visualize dynamic EEG graphs in an example EEG clip in the TUSZ test set, inferred by the GSL layer. In the beginning of the EEG clip (Figures 6a–6d), the seizure starts as a focal seizure and the corresponding EEG graphs are sparse. Starting at the last 2-s of Figure 6e, the seizure starts to spread. In the last 10-s of this EEG clip (Figure 6f), the seizure spreads to all areas of the brain and the EEG graph becomes denser with more edges than the earlier EEG graphs. This change in graph connectivity reflects the dynamics of the seizure.

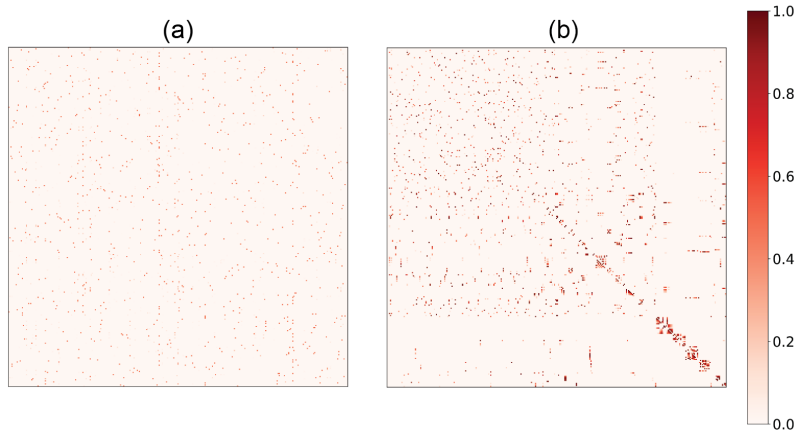


Figure 5: (a) Mean adjacency matrix for traffic forecasting inferred by our GSL layer. (b) Adjacency matrix in Li et al. [45] constructed based on traffic sensor locations. Self-edges (i.e., diagonal) are not shown here.

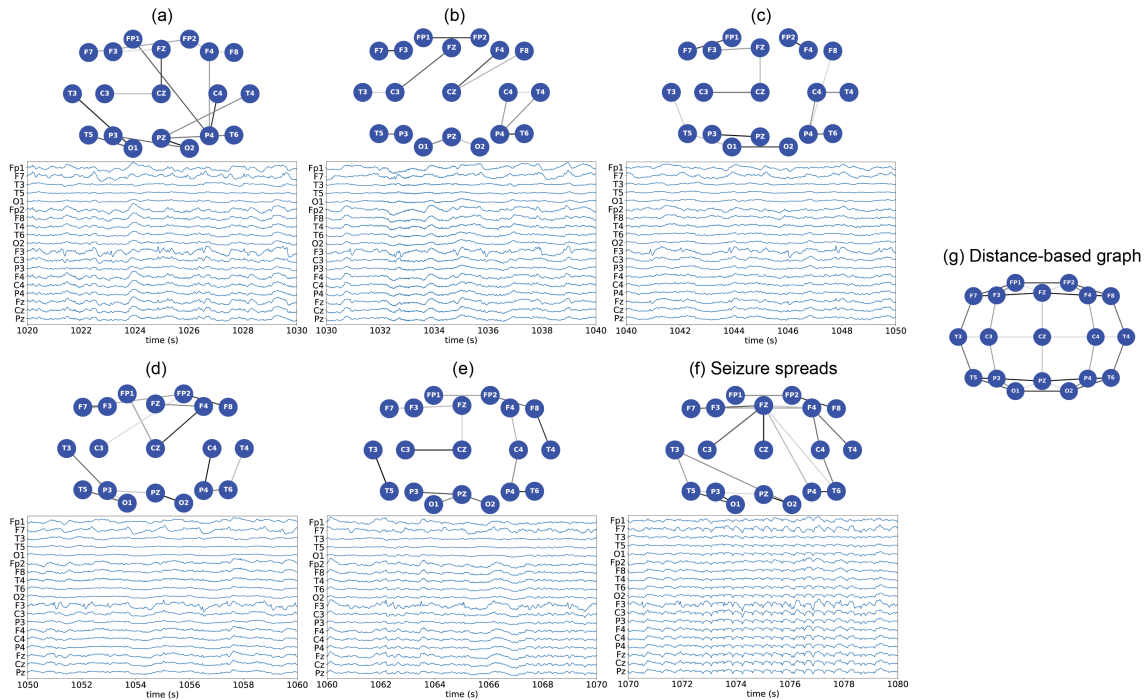


Figure 6: **Example EEG graphs of a 60-s EEG clip that has seizure in the test set.** In each subfigure in (a)–(f), top panel shows the inferred graph from the GSL layer and bottom panel shows the raw EEG signals. (g) Distance-based graph in Tang et al. [66], defined based on physical distances between EEG sensors in the standard 10-20 EEG placement system.